

Tuning the Nature and Formation of Bis(dihydrogen)-Osmium Species

Miguel A. Esteruelas,* M. Pilar Gay, Virginia Lezáun, Montserrat Oliván, and Enrique Oñate

Departamento de Química Inorgánica – Instituto de Síntesis Química y Catálisis Homogénea (ISQCH) – Centro de Innovación en Química Avanzada (ORFEO-CINQA), Universidad de Zaragoza – CSIC, 50009 Zaragoza, Spain

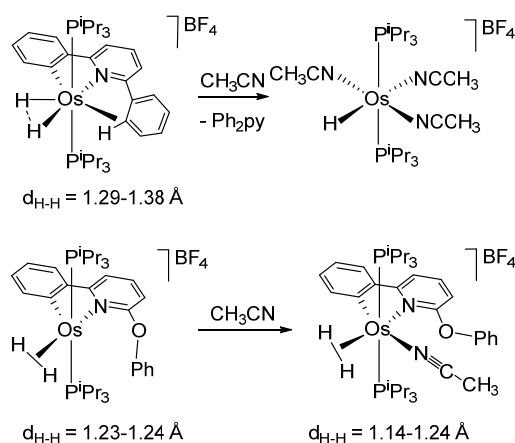
Supporting Information Placeholder

ABSTRACT: The influence of chelate ligands in the formation and nature of bis(dihydrogen) units of OsH₄-complexes has been studied. The classical trihydride OsH₃{κ²-C,N-(C₆H₄-py)}(PⁱPr₃)₂ (**1**) reacts with HBF₄·OEt₂ to give the Kubas-type dihydrogen-elongated dihydrogen derivative [Os{κ²-C,N-(C₆H₄-py)}(η²-H₂)₂(PⁱPr₃)₂]BF₄ (**2**), as a result of the protonation of one of the hydride ligands. Triflate (OTf) displaces the Kubas-type dihydrogen and elongates the elongated dihydrogen ligand, which is converted into a compressed dihydride. Thus, the addition of one equiv of HOTf to **1** leads to Os(H···H){κ²-C,N-(C₆H₄-py)}(OTf)(PⁱPr₃)₂ (**3**). Similarly to [OTf], acetone reacts with **2** to afford the related compressed dihydride [Os(H···H){κ²-C,N-(C₆H₄-py)}(κ¹-OCMe₂)(PⁱPr₃)₂]BF₄ (**4**), whereas acetonitrile leads to a 1:8 mixture of the monohydride [OsH(CH₃CN)₃(PⁱPr₃)₂]BF₄ (**5**) and the trihydride [OsH₃(CH₃CN)₂(PⁱPr₃)₂]BF₄ (**6**). Reactions of **2** with toluene and *p*-xylene yield the half-sandwich derivatives [Os{κ²-C,N-(C₆H₄-py)}(η⁶-toluene)(PⁱPr₃)₂]BF₄ (**7**) and [Os{κ²-C,N-(C₆H₄-py)}(η⁶-*p*-xylene)(PⁱPr₃)₂]BF₄ (**8**), respectively. The acyl oxygen atom of the C,C-chelate ligand of the trihydride OsH₃{κ²-C,C-[C(O)CH₂ImMe]}(PⁱPr₃)₂ (**10**; Im = imidazolylidene) provides reliable and effective protection of the hydride ligands against the protonation. Thus, the addition of HBF₄·OEt₂ or HOTf to **10** leads to the trihydride-hydroxycarbene cation [OsH₃{κ²-C,C-[C(OH)CH₂ImMe]}(PⁱPr₃)₂]⁺ (**11**). The hydroxycarbene-NHC ligand of the latter is unstable, undergoing an intramolecular 1,3-hydrogen shift, which produces the rupture of the chelate ligand and the formation of the *cis*-hydride dihydrogen (**12a**) and *trans*-hydride-dihydrogen (**12b**) derivatives [OsH(η²-H₂)(CO)(Me₂Im)(PⁱPr₃)₂]⁺ (**12**). The protonation of **11** with a second equiv of HOTf affords the transient bis(Kubas-type dihydrogen) [Os(η²-H₂)₂{κ²-C,C-[C(OH)CH₂ImMe]}(PⁱPr₃)₂](OTf)₂, which undergoes the displacement of a coordinated hydrogen molecule by a [OTf] anion to give the Kubas-type dihydrogen [Os(OTf)(η²-H₂){κ²-C,C-[C(OH)CH₂ImMe]}(PⁱPr₃)₂]OTf (**13**). The addition of MeOTf to **10** leads to [OsH₃{κ²-C,C-[C(OMe)CH₂ImMe]}(PⁱPr₃)₂]OTf (**14**) which, in contrast to **11**, is stable. Similarly to the latter, the protonation of **14** with HOTf yields the Kubas-type dihydrogen complex [Os(OTf)(η²-H₂){κ²-C,C-[C(OMe)CH₂ImMe]}(PⁱPr₃)₂]OTf (**15**).

INTRODUCTION

Chemistry of transition metal complexes is ligand dependent. Probably, nothing illustrates that better than polyhydrides of platinum group metals.¹ Ligands have under control the interactions between the coordinated hydrogen atoms and between the latter and the metal center. According to their strength, the compounds are classified in four classes: classical hydrides (>1.6 Å), compressed dihydrides (1.6-1.3 Å), elongated dihydrogen (1.3-1.0 Å) and Kubas-type dihydrogen (1.0-0.8 Å).^{1,2,3} Although the limits between them are vague, recent studies have demonstrated that the compounds of each class have different chemical nature and therefore different chemical behavior. Thus, for instance, we have recently shown that the compressed dihydride [OsH₂(C₆H₄pyPh)(PⁱPr₃)₂]BF₄ eliminates 2,6-diphenylpyridine in acetonitrile, while the elongated dihydrogen [Os(C₆H₄pyOPh)(η²-H₂)(PⁱPr₃)₂]BF₄ is stable toward the release of 2-phenoxy-6-phenylpyridine, under the same conditions (Scheme 1).⁴

Scheme 1. Compressed Dihydride versus Elongated Dihydrogen



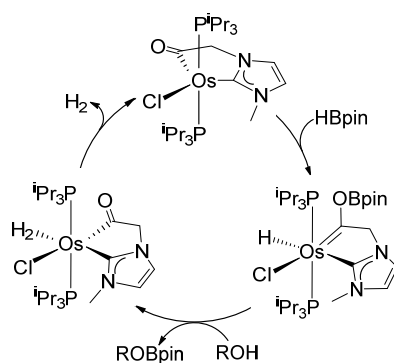
Osmium-polyhydrides occupy a prominent place among the compounds of this type, because of OsH_n-species offer new conceptual challenges and show notable applications in organometallics,⁵ catalysis,⁶ drug design,⁷ and material sci-

ence.⁸ The OsH₄-compounds are particularly exciting. They have been grouped into classical tetrahydrides,⁹ dihydride-dihydrogen derivatives,¹⁰ and bis(dihydrogen) species.¹¹ The latter are the most interesting from a conceptual point of view, without a shadow of a doubt, and also the scarcest. With the notable exception of complex [Os(η²-H₂)₂(PGP)]BPh₄ (PGP = κ⁴-^tBu₂PCH₂CH{N(Me)CH=}CH(CH₂)₂P^tBu₂), which has been described as a bis(elongated dihydrogen) species with two equal H-H bonds of 1.11 Å,^{11b} both coordinated molecules form Kubas-type dihydrogen ligands which can be sequentially displaced by coordinating solvents.^{11a,d} In this context, it should be however mentioned that the behavior of this type of compounds in usual organic solvents has been little studied.

One of the most direct and simple procedures to prepare OsH₄-complexes is the protonation of trihydride derivatives. For terdentate ligands, it has been proved that the nature of the resulting species depends upon the geometry of these groups. Thus, while hydridotris(pyrazolyl)borate- and bis(2-aminoethyl)amine-type ligands favor octahedral osmium(II)-bis(dihydrogen) derivatives with N-Os-N angles close to the ideal value of 90°,^{11a,c} cyclopentadienyl,^{10c} pentamethylcyclopentadienyl,^{10b,d} 1,4,7-triazacyclononane, and 1,4,7-triazacyclodecane^{11c} stabilize dihydride–elongated dihydrogen–osmium(IV) species in four-legged piano stool or pentagonal bipyramidal environments. The protonation of trihydride compounds containing a bidentate ligand has received significantly less attention; in part due to the lower stability of the resulting cationic OsH₄-species.¹²

There is a type of ligands that have received great attention in the last years, in particular in homogeneous catalysis, those called cooperative. The presence of free electrons in a non-coordinated atom allows them to participate directly in a σ-bond activation stage and subsequently to perform a reversible structural change in the process of product formation.¹³ An example is the acyl-NHC ligand of complex OsCl{κ²-C,C-[C(O)CH₂ImMe]}(PⁱPr₃)₂ (Im = imidazolylidene), which catalyzes the generation of H₂, by means of both the alcoholysis and hydrolysis of pinacolborane (Scheme 2).¹⁴

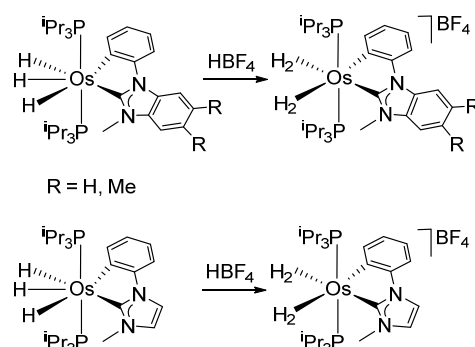
Scheme 2. Alcoholysis of Pinacolborane Catalyzed by OsCl{κ²-C,C-[C(O)CH₂ImMe]}(PⁱPr₃)₂



Our interest in the reactions of protonation of osmium(IV)-trihydride complexes, prompted us to compare the protonation of trihydride derivatives with chelate observer-type groups, which subtly govern the nature of the resulting species without participating directly in the process, with the protonation of a trihydride derivative containing this acyl-NHC ligand, in order to know the behavior of the basic heteroatom and to determine

the role of the acyl group in the formation of the resulting species. As chelate observer-type ligands, we selected an orthometalated 2-phenylpyridine group and the aryl-NHC ligands of complexes OsH₃{κ²-C_{aryl},C_{NHC}}(PⁱPr₃)₂. The latter have proven to stabilize bis(Kubas-type dihydrogen) derivatives (Scheme 3).^{11d}

Scheme 3. Synthesis of Bis(dihydrogen) Derivatives Stabilized by aryl-NHC Ligands



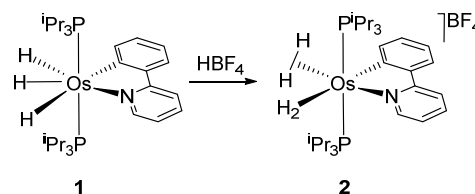
This paper shows that chelating ligands, which act as a spectator, determine the behavior in solution of the osmium-bis(dihydrogen) complexes whereas the oxygen atom of the acyl-NHC ligand prevents their formation. In addition, we report the first Kubas-type dihydrogen–elongated dihydrogen osmium derivative and the first hydride compounds displaying nonclassical interactions which are stabilized by Fisher-type carbene ligands.

RESULTS AND DISCUSSION

Formation of a Kubas-type Dihydrogen–Elongated Dihydrogen Complex: Protonation of a Trihydride Compound Containing an Orthometalated 2-Phenylpyridine Group.

Classical trihydride OsH₃{κ²-C,N-(C₆H₄-py)}(PⁱPr₃)₂ (**1**) is a Brønsted base. At least one of its hydride ligands is responsible for this character. At room temperature the addition of 1.0 equiv of HBF₄·OEt₂ to dichloromethane solutions of **1** produces the protonation of one of the hydride ligands. The addition is accompanied by the reduction of the metal center from osmium(IV) to osmium(II). Both processes give rise to the Kubas-type dihydrogen–elongated dihydrogen derivative [Os{κ²-C,N-(C₆H₄-py)}(η²-H₂)₂(PⁱPr₃)₂]⁺BF₄⁻ (**2**), which was isolated as a yellow solid in 85% yield (Scheme 4).

Scheme 4. Protonation of Complex 1 with HBF₄·OEt₂



Complex **2** has been characterized by X-ray diffraction. Figure 1a shows a view of the cation of the salt. The coordination polyhedron around the osmium atom is the expected octahedron for a saturated d⁶-species, with *trans*-phosphines (P(1)-Os-P(1A) = 163.07(4)°). The perpendicular plane is

formed by the chelate ligand, which acts with a C(1)-Os-N(1) bite angle of $77.46(17)^\circ$ and the dihydrogen ligands. The orientation of the latter with regard to the P-Os-P direction depend upon the donor atom situated *trans* to the coordinated H₂ molecule. The dihydrogen ligand disposed *trans* to the nitrogen atom (H(01)-H(02)) lies in the perpendicular plane along with the C,N-chelate ligand, with the hydrogen atoms separated by 1.13(6) Å, whereas that situated *trans* to the carbon atom (H(03)-H(03A)) is disposed almost parallel to the P-Os-P direction, with the hydrogen atoms separated by 0.88(2) Å. The DFT-optimized structure (Figure 1b) confirms the non-classical interaction between the hydrogen atoms bonded to the metal center and the Kubas-type dihydrogen-elongated dihydrogen character of the OsH₄ unit. The calculated values for the H-H bond lengths agree well with those obtained by X-ray diffraction analysis. According to them, the nature of H(01)-H(02) (0.989 Å) appears to be an elongated dihydrogen, which lies in the border with a Kubas-type dihydrogen, while H(03)-H(03A) (0.886 Å) is a Kubas-type dihydrogen.

The ¹H NMR spectrum of **2**, in dichloromethane-*d*₂, is temperature dependent. Between 283 and 213 K, the dihydrogen ligands give rise to a broad resonance centered at -7.2 ppm which display a 300 MHz *T*₁(min) value of 21 ± 3 ms at 243 K, supporting the nonclassical interaction between the hydrogen atoms coordinated to the metal center also in solution. The presence of only one resonance for the inequivalent dihydrogen ligands indicates that they are involved in a thermally activated exchange process. Thus, at 203 K, decoalescence occurs and at temperatures lower than 193 K two broad resonances centered at -3.6 and -11.0 ppm are clearly observed. According with these data, the estimated activation energy (ΔG^\ddagger) for the exchange is 8.3 kcal·mol⁻¹, which may be related to the activation energy for the oxidative addition of H(01)-H(02) to the metal center to afford a dihydride-dihydrogen intermediate. This type of species could change the position of the hydrogen atoms coordinated to the osmium atom by combining both proton transfer and dihydride-dihydrogen tautomerization processes (Scheme 5). Attempts to obtain a *J*_{H-D} value were unsuccessful, which is common for L_nMH_m polyhydrides where *m* > 2.^{2b} The fluxionality in polyhydrides, which makes the measurement impossible, is a complex problem.¹ It could involve the conversion dihydride – dihydrogen as in complex **2**, a change in the geometry of the complex without modifying the interactions in the MH_m units, position exchanges of hydrogen atoms in a concerted manner due to the high mobility of hydrogen atoms in the coordination sphere of the metal¹⁵ or proton transfer. In contrast to the ¹H NMR spectrum, the ³¹P{¹H} NMR spectrum is temperature invariant. In agreement with the presence of equivalent phosphines, it shows a singlet at 13.9 ppm. In the ¹³C{¹H} NMR spectrum the most noticeable feature is a triplet (²*J*_{C-P} = 10.7 Hz) at 150.5 ppm due to the metalated carbon atom C(1) of the chelate ligand.

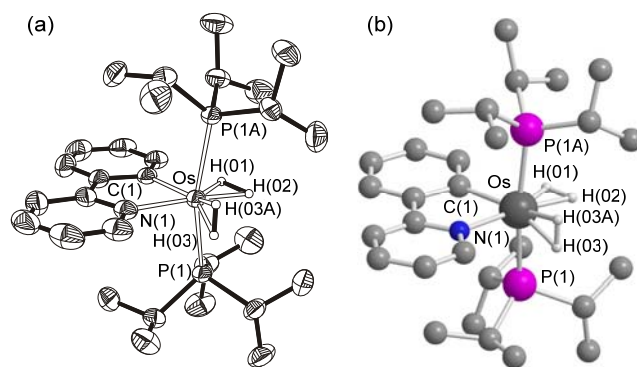
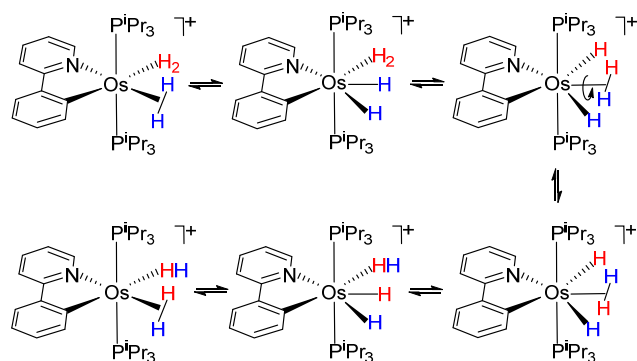


Figure 1. (a) ORTEP diagram of the cation of complex **2** (50% probability ellipsoids). Most hydrogen atoms are omitted for clarity. Selected bond lengths (Å) and angles (deg): Os-P(1) = 2.4003(10), Os-N(1) = 2.140(4), Os-C(1) = 2.103(4), H(01)-H(02) = 1.13(6), H(03)-H(03A) = 0.88(2); P(1)-Os-P(1A) = 163.07(4), N(1)-Os-C(1) = 77.46(17). (b) Optimized structure of the cation of complex **2**. Most hydrogen atoms are omitted for clarity. Selected bond lengths (Å) and angles (deg): Os-P(1) = 2.456, Os-P(1A) = 2.452, Os-N(1) = 2.136, Os-C(1) = 2.099, H(01)-H(02) = 0.989, H(03)-H(03A) = 0.886; P(1)-Os-P(1A) = 169.3, N(1)-Os-C(1) = 78.0.

Scheme 5. Position exchange of the Hydrogen Atoms Coordinated to the Metal Center of **2**



The protonation of **1** is a reaction that depends upon the conjugated base of the used Brønsted acid. In contrast to HBF₄·OEt₂, triflic acid (HOTf) affords H₂ and the neutral compressed dihydride Os(H···H){κ²-C,N-(C₆H₄-py)}(OTf)(PⁱPr₃)₂ (**3**). The addition of the proton of the acid to one of the hydride ligands of **1** initially gives **2**, which subsequently undergoes the displacement of the Kubas-type dihydrogen by the triflate anion and the elongation of the elongated dihydrogen. Complex **3** was isolated as a yellow solid in 87% yield, according to Scheme 6, and characterized by X-ray diffraction analysis.

Scheme 6. Protonation of Complex 1 with HOTf.

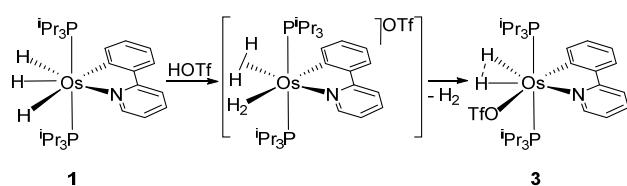


Figure 2a shows a view of the structure of the molecule, which resembles that of **2** with the triflate anion in the position of the Kubas-type dihydrogen and the coordinated hydrogen atoms H(01) and H(02) separated by 1.41(7) Å. Thus, the coordination polyhedron around the osmium atom can be rationalized as a distorted pentagonal bipyramid with the phosphines in apical positions (P(1)-Os-P(2) = 166.42(8)°) and the triflate anion situated in the perpendicular plane forming an O(1)-Os-C(1) angle of 161.2(2)° with the metalated carbon atom of the orthometalated phenylpyridine ligand. The DFT-optimized structure confirms that the replacement of the Kubas-type dihydrogen of **2** by the triflate anion produces a significant separation between H(01) and H(02). Thus, the value obtained for **3** of 1.352 Å is 0.363 Å longer than the obtained one for **2**. The elongation is also supported by the ¹H NMR spectrum in dichloromethane-*d*₂, which shows a triplet (²*J*_{H-P} = 10.6 Hz) at -7.04 ppm for the coordinated hydrogen atoms. According to their nonclassical nature, this resonance exhibits a 300 MHz *T*₁(min) value of 28 ± 1 ms, at 213 K, which allows to calculate a separation between H(01) and H(02) of 1.25 Å,¹⁶ although slightly shorter than those obtained by X-ray diffraction analysis and DFT-calculations, significantly longer than the H(01)-H(02) bond length in **2**. The ³¹P{¹H} NMR spectrum shows a singlet at 7.6 ppm, in agreement with the equivalence of the phosphines. In the ¹³C{¹H} NMR spectrum, the metalated carbon atom C(1) displays a triplet (²*J*_{C-P} = 5.5 Hz) at 158.8 ppm.

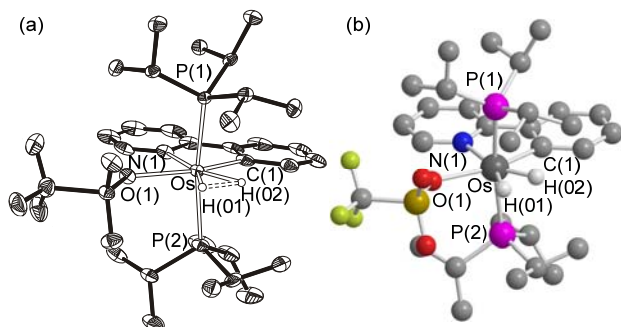


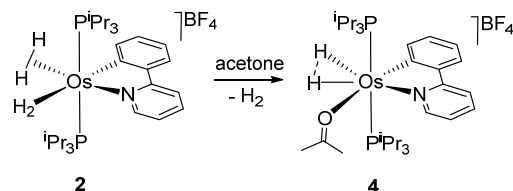
Figure 2. (a) ORTEP diagram of complex **3** (50% probability ellipsoids). Most hydrogen atoms are omitted for clarity. Selected bond lengths (Å) and angles (deg): Os-P(1) = 2.3950(11), Os-P(2) = 2.4059(15), Os-N(1) = 2.151(5), Os-C(1) = 2.043(6), Os-O(1) = 2.260(4), H(01)-H(02) = 1.41(7); P(1)-Os-P(2) = 166.42(8), N(1)-Os-C(1) = 78.1(3), N(1)-Os-O(1) = 83.13(18), C(1)-Os-O(1) = 161.2(2). (b) Optimized structure of complex **3**. Most hydrogen atoms are omitted for clarity. Selected bond lengths (Å) and angles (deg): Os-P(1) = 2.423, Os-P(2) = 2.423, Os-N(1) = 2.201, Os-C(1) = 2.070, H(01)-H(02) = 1.352; P(1)-Os-P(2) = 167.6, N(1)-Os-C(1) = 77.1.

Behavior of 2 in Usual Organic Solvents. Cations [Os(κ²-C_{aryl}-C_{NHC})(η²-H₂)₂(PⁱPr₃)₂]⁺ shown in Scheme 3 are bis(Kubas-type dihydrogen) species. However, X-ray diffraction analysis and DFT calculations data support a Kubas-type dihydrogen-elongated dihydrogen formulation for **2**. This apparent subtlety gives rise to a marked difference in reactivity between the bis(dihydrogen) derivatives shown in Scheme 3 and complex **2**, which is revealed by their different behavior in usual organic solvents, such as acetone and acetonitrile, although they are stable in dichloromethane.

Atoms in Molecules (AIM) and Natural Bond Orbitals (NBO) methods have revealed that the Os-C_{NHC} bond in the cations shown in Scheme 3 has a significant π-contribution due to the π-acceptor ability of the p_z orbital at the C_{NHC} atom.^{11d} As a consequence of the remarkable π-backdonation to C_{NHC}, the backdonation of the metal center to the hydrogen molecule situated *trans* to C_{NHC} decreases, whereas the σ-donation of the coordinated H-H bond to the osmium is stimulated, increasing the polarization of the bond and therefore the Brønsted acidity of the coordinated molecule.¹⁷ Thus, cations [Os(κ²-C_{aryl}-C_{NHC})(η²-H₂)₂(PⁱPr₃)₂]⁺ display acidities similar to phosphoric acid and organic compounds such as bromoacetic acid or chloroacetic acid, which allow the protonation of acetone. In this solvent, the cations reverse to the trihydrides OsH₃(κ²-C_{aryl}-C_{NHC})(PⁱPr₃)₂.^{11d}

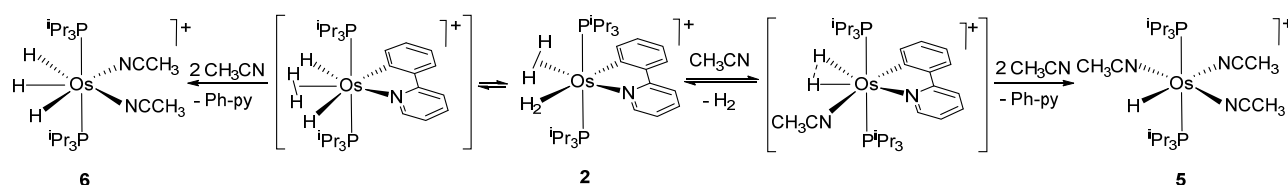
The nitrogen atom of pyridine does not show the π-acceptor ability of C_{NHC}. Thus, in contrast to [Os(κ²-C_{aryl}-C_{NHC})(η²-H₂)₂(PⁱPr₃)₂]⁺, complex **2** loses the Kubas-type dihydrogen and the solvent occupies its position. Like in the [OTf]⁻ case, the substitution produces the elongation of the elongated dihydrogen which is converted into a compressed dihydride. The resulting species [Os(H⋯H){κ²-C_N(C₆H₄-py)}(κ¹-OCMe₂)(PⁱPr₃)₂][BF₄ (**4**) was isolated as a green solid in almost quantitative yield (Scheme 7). The compressed dihydride character of the OsH₂-unit is supported by the ¹H NMR spectrum, in dichloromethane-*d*₂, of the obtained solid, which contains a broad signal at -7.21 ppm. This resonance exhibits a 300 MHz *T*₁(min) value of 33 ± 1 ms, at 213 K, which allows to calculate¹⁶ a separation between the coordinated hydrogen atoms of 1.29 Å. The optimized DFT-structure of **4** yields a value of 1.329 Å, confirming the compressed dihydride character of the species. The ³¹P{¹H} NMR spectrum shows a singlet at 6.1 ppm, for the equivalent phosphines. In the ¹³C{¹H} NMR spectrum, the resonance corresponding to the metalated carbon atom of the C_N chelate ligand appears at 154.4 ppm as a triplet with a C-P coupling constant of 7.1 Hz.

Scheme 7. Reaction of Complex 2 with Acetone



Acetone and acetonitrile give rise to very different behaviors. Cations [Os(κ²-C_{aryl}-C_{NHC})(η²-H₂)₂(PⁱPr₃)₂]⁺ do not undergo deprotonation in acetonitrile. In contrast to acetone, this solvent displaces the coordinated hydrogen molecules to afford the corresponding [Os(κ²-C_{aryl}-C_{NHC})(CH₃CN)₂(PⁱPr₃)₂]⁺

Scheme 8. Reaction of Complex 2 with Acetonitrile



bis(solvento) compounds.^{11d} Under the same conditions, complex **2** eliminates 2-phenylpyridine to give a 1:8 mixture of the monohydride $[\text{OsH}(\text{CH}_3\text{CN})_3(\text{P}^i\text{Pr}_3)_2]\text{BF}_4$ (**5**) and the trihydride $[\text{OsH}_3(\text{CH}_3\text{CN})_2(\text{P}^i\text{Pr}_3)_2]\text{BF}_4$ (**6**).¹⁸ The reaction, which can be rationalized according to Scheme 8, is consistent with the marked ability of the orthometalated 2-phenylpyridine group to form compressed dihydride species. According to this ability, the displacement of the Kubas-type dihydrogen of **2** by an acetonitrile molecule should give a compressed dihydride intermediate analogous to **4**, which could evolve by reductive elimination of 2-phenylpyridine.⁴ The trapping of the resulting $14 e^-$ valence fragment $[\text{OsH}(\text{CH}_3\text{CN})(\text{P}^i\text{Pr}_3)_2]^+$ by the solvent should yield **5**. The trihydride **6** could result from the reductive elimination of 2-phenylpyridine via a dihydride-dihydrogen intermediate as those shown in Scheme 5 and the subsequent trapping of the generated metal fragment $[\text{OsH}_3(\text{P}^i\text{Pr}_3)_2]^+$ by the solvent.

Complex **2** is insoluble in aromatic solvent such as toluene and *p*-xylene, in agreement with their low polarity and the saline character of the complex. The heating of the suspensions produces the release of the coordinated hydrogen molecules. The unsaturated metal center is stabilized by the solvent, which displaces one of the phosphine ligands to afford the half-sandwich cations $[\text{Os}\{\kappa^2\text{-C},N\text{-}(\text{C}_6\text{H}_4\text{-py})\}(\eta^6\text{-toluene})(\text{P}^i\text{Pr}_3)]^+$ (**7**) and $[\text{Os}\{\kappa^2\text{-C},N\text{-}(\text{C}_6\text{H}_4\text{-py})\}(\eta^6\text{-}p\text{-xylene})(\text{P}^i\text{Pr}_3)]^+$ (**8**), according to Scheme 9. These cations can be also obtained starting from **3**, which is soluble in the aromatic solvents. The $[\text{OTf}]$ salts were isolated as yellow solids in good yield, 60-70%.

Scheme 9. Reaction of Complex 2 with Aromatic Solvents

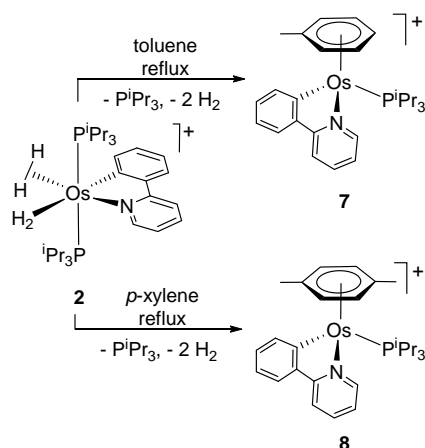


Figure 3 shows a view of the cation of **7**. The geometry around the osmium atom is close to octahedral, with the arene occupying three sites of a face. In agreement with the presence

of the phosphine ligand, the $^{31}\text{P}\{^1\text{H}\}$ NMR spectra, in dichloromethane- d_2 , show a singlet at 3.3 ppm for **7** and -1.7 ppm for **8**. In the $^{13}\text{C}\{^1\text{H}\}$ NMR spectra the resonance due to the metalated carbon atom of the C,N-ligand is observed as a doublet ($^2J_{\text{C-P}} = 13.6$ Hz) at about 159 ppm.

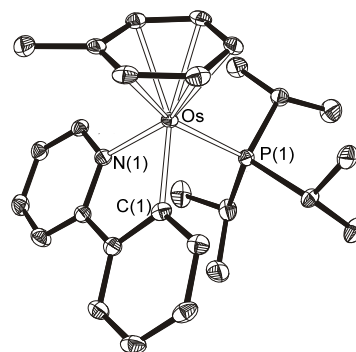
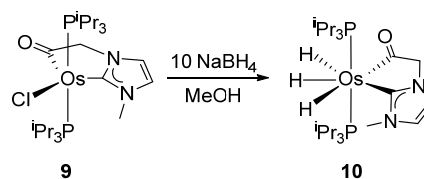


Figure 3. ORTEP diagram of the cation of complex **7** (50% probability ellipsoids). Hydrogen atoms are omitted for clarity. Selected bond lengths (Å) and angles (deg): Os-P(1) = 2.3821(8), Os-N(1) = 2.088(2), Os-C(1) = 2.066(3); P(1)-Os-N(1) = 92.60(7), P(1)-Os-C(1) = 87.08(8), N(1)-Os-C(1) = 77.72(10).

Preparation of $\text{OsH}_3\{\kappa^2\text{-C},C\text{-}[\text{C}(\text{O})\text{CH}_2\text{ImCH}_3]\}(\text{P}^i\text{Pr}_3)_2$ (10**).** A straightforward procedure for the preparation of polyhydride complexes of platinum group metals, which has proved to be particularly useful in the osmium chemistry is the alcoholysis of tetrahydrideborate derivatives. These compounds are generally generated in situ, by replacement of a chloride ligand by a $[\text{BH}_4]$ group.¹⁹

The procedure has been also successful in this case. At room temperature, the treatment of toluene solutions of the chloride-acyl-NHC complex $\text{OsCl}\{\kappa^2\text{-C},C\text{-}[\text{C}(\text{O})\text{CH}_2\text{ImMe}]\}(\text{P}^i\text{Pr}_3)_2$ (**9**) with 10 equiv of NaBH_4 and subsequently with methanol added drop by drop leads to the wished trihydride $\text{OsH}_3\{\kappa^2\text{-C},C\text{-}[\text{C}(\text{O})\text{CH}_2\text{ImMe}]\}(\text{P}^i\text{Pr}_3)_2$ (**10**), which was isolated as a white solid in 42% yield (Scheme 10).

Scheme 10. Synthesis of Complex 10.



Complex **10** was characterized by X-ray diffraction analysis. Figure 4a gives a view of the molecule. The coordination geometry around the osmium atom can be described as a distorted pentagonal bipyramid with axial phosphines (P(1)-Os-P(2) = 169.433(19) $^\circ$). The metal coordination sphere is completed by the hydride ligands, separated by 1.58(4) (H(01) and H(02)) and 1.77(3) (H(02) and H(03)) Å, and the carbon atoms of the acyl-NHC group, which act with a C(1)-Os-C(6) bite angle of 77.30(8) $^\circ$. The Os-NHC and Os-acyl distances of 2.086(2) (Os-C(1)) and 2.115(2) (Os-C(6)) Å, respectively, compare well with those previously reported for other Os $\{\kappa^2\text{-C,C-[C(O)CH}_2\text{ImMe}\}\}$ -complexes.¹⁴ The classical trihydride nature of the complex was confirmed by the DFT-optimized structure (Figure 4b), which affords separations between the hydrides of 1.734 and 1.778 Å.

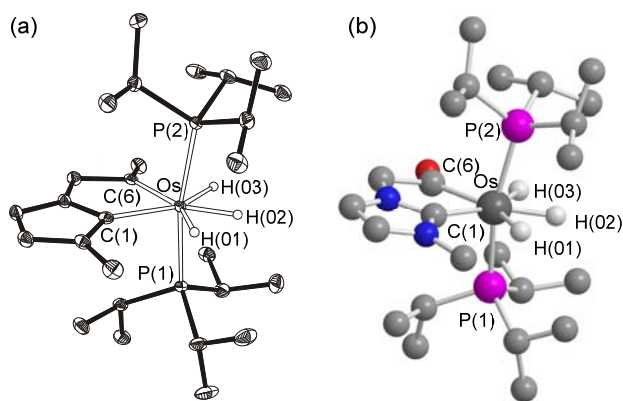


Figure 4. (a) ORTEP diagram of complex **10** (50% probability ellipsoids). Hydrogen atoms (except the hydrides) are omitted for clarity. Selected bond lengths (Å) and angles (deg): Os-P(1) = 2.3550(5), Os-P(2) = 2.3501(6), Os-C(1) = 2.086(2), Os-C(6) = 2.115(2), H(01)-H(02) = 1.58(4), H(02)-H(03) = 1.77(3); P(1)-Os-P(2) = 169.433(19), C(1)-Os-C(6) = 77.30(8). (b) Optimized structure of complex **10**. Hydrogen atoms (except the hydrides) are omitted for clarity. Selected bond lengths (Å) and angles (deg): Os-P(1) = 2.379, Os-P(2) = 2.375, Os-C(1) = 2.106, Os-C(6) = 2.149, H(01)-H(02) = 1.734, H(02)-H(03) = 1.778; P(1)-Os-P(2) = 166.0, C(1)-Os-C(6) = 76.8.

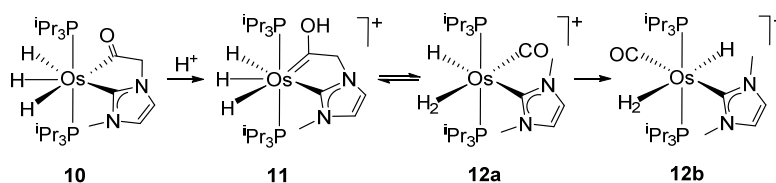
The $^{31}\text{P}\{^1\text{H}\}$, $^{13}\text{C}\{^1\text{H}\}$ and ^1H NMR spectra in toluene- d_8 are consistent with the structure shown in Figure 4a. In agreement with the presence of equivalent phosphines, the $^{31}\text{P}\{^1\text{H}\}$ NMR spectrum contains a singlet at 29.9 ppm. In the $^{13}\text{C}\{^1\text{H}\}$ NMR spectrum, the C(1)-NHC and C(6)-acyl resonances are observed at 188.9 and 255.9 ppm, as triplets with C-P coupling constants of 6.4 and 7.9 Hz, respectively. The ^1H NMR spectrum at 183 K shows three high-field resonances centered at -8.1, -10.9 and -11.2 ppm, in a 1:1:1 intensity ratio, as expected for three inequivalent hydride ligands. The signals at -10.9 and -11.2 ppm coalesce between 203 and 213 K to afford a broad signal. The latter coalesces with the resonance at -8.1 ppm, between 283 K and 293 K, to yield only one hydride resonance at temperatures higher than 293 K. This behavior indicates two thermally activated site exchange processes involving to H(01) and H(02) and the latter with H(03), which occur with activation energies of about 9.7 kcal·mol $^{-1}$ and 12.5 kcal·mol $^{-1}$, respectively. According to the presence of the acyl group, the IR shows a characteristic $\nu(\text{CO})$ band at 1556 cm $^{-1}$.

Protonation of 10. There are marked differences in behavior between **1** and **10**. The acyl oxygen atom of the C,C-chelate ligand of the latter provides reliable and effective protection to the hydride ligands against the protonation with both $\text{HBF}_4\cdot\text{OEt}_2$ and HOTf and allows the preparation of the first transition metal complexes containing a chelate ligand formed by an NHC unit and an oxygen substituted Fischer-type carbene moiety. The addition of 1.0 equiv of the above mentioned acids to the dichloromethane- d_2 solutions of **10** at room temperature leads to the quantitative formation of the trihydride hydroxycarbene cation $[\text{OsH}_3\{\kappa^2\text{-C,C-[C(OH)CH}_2\text{ImMe}\}\}(\text{P}^i\text{Pr}_3)_2]^+$ (**11**), as result of the protonation of the acyl oxygen atom (Scheme 11). The addition of the proton of the acids to the acyl oxygen atom is strongly supported by the ^1H NMR spectrum of the resulting solution, which contains an OH-resonance at 13.53 ppm. In the high field region, the hydride ligands give rise to a triplet ($J_{\text{H-P}} = 11.7$ Hz) at -8.89 ppm, which displays a 400 MHz $T_1(\text{min})$ value of 112 ± 5 ms, at 203 K, in agreement with the classical character of the OsH_3 -unit. The $^{31}\text{P}\{^1\text{H}\}$ NMR spectrum shows a singlet at 30.0 ppm.

The hydroxycarbene-NHC ligand of **11** is unstable, undergoing an intramolecular 1,3-hydrogen shift from the oxygen atom to the methylene moiety. The migration produces the decarbonylation of the C,C-chelate ligand, which is converted into a carbonyl group and a N,N-dimethylimidazolylidene ligand. The decarbonylation is accompanied by the reduction of the metal center and the transformation of the classical trihydride into hydride-dihydrogen. The resulting cation $[\text{OsH}(\eta^2\text{-H}_2)(\text{CO})(\text{Me}_2\text{Im})(\text{P}^i\text{Pr}_3)_2]^+$ (**12**) exists as two isomers: *cis*-hydride-dihydrogen (**12a**, $J_{\text{H-D}} = 28.0$; H-H = 0.95 Å) and *trans*-hydride-dihydrogen (**12b**, $J_{\text{H-D}} = 26.6$; H-H = 0.98 Å). Isomer **12a** is the kinetically controlled product, while isomer **12b** is the most stable. Thus, after 12 h, it is the main species in solution. Characteristic spectroscopic data of **12a** are: the OsH_3 -resonance in the ^1H NMR spectrum, which appears at -6.2 ppm, as a broad signal, and displays a 300 MHz $T_1(\text{min})$ value of 10 ± 1 ms, at 203 K, and a singlet at 15.2 ppm in the $^{31}\text{P}\{^1\text{H}\}$ NMR spectrum due to the equivalent phosphines. In contrast to **12a**, the hydride-dihydrogen unit of **12b** originates two resonances in the ^1H NMR spectrum, a broad signal at -5.44 ppm corresponding to the coordinated hydrogen molecule and a triplet ($^2J_{\text{H-P}} = 21.9$ Hz) at -6.08 ppm due to the hydride ligand. The first of them shows a 300 MHz $T_1(\text{min})$ value of 14 ± 1 ms, whereas the 300 MHz $T_1(\text{min})$ value of the second one is 266 ± 13 ms. Both values were obtained at 223 K. In the $^{13}\text{C}\{^1\text{H}\}$ NMR spectrum, the CO resonance is observed at 182.1 ($^2J_{\text{C-P}} = 9.8$ Hz) ppm, whereas the signal due to the metalated carbon atom of the NHC ligand appears at 163.1 ($^2J_{\text{C-P}} = 8.3$ Hz) ppm. A singlet at 31.4 ppm in the $^{31}\text{P}\{^1\text{H}\}$ NMR spectrum is also a characteristic feature of this species.

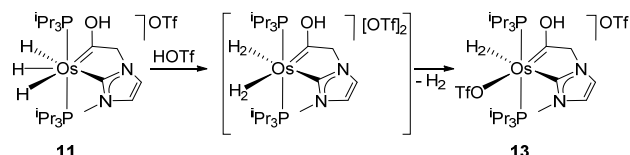
NHC carbene ligands are recognized as powerful tools in organometallic and catalysis, due to their robustness.²⁰ However findings reported in recent years reveal that they can undergo degradation via σ -bond activation reactions on their substituents.²¹ The transformation of **11** into **12** constitutes a new evidence in this line. The cleavage of C-C bonds is the less frequent among the metal-mediated σ -bond activation processes. One of the driving forces to promote the reaction is the stabilization of the resulting metal species by chelate effect.^{7e,22} In this context it should be noted that in contrast to the general trend the C-C cleavage that transforms **11** into **12** implies the rupture of a chelating system.

Scheme 11. Protonation of Complex 10



Once the basicity of the acyl oxygen atom has been neutralized, the hydride ligands are susceptible to being protonated. Thus, the addition of a second equivalent of HOTf to dichloromethane solutions of **11** affords the Kubas-type dihydrogen derivative $[\text{Os}(\text{OTf})(\eta^2\text{-H}_2)\{\kappa^2\text{-C,C-}[\text{C}(\text{OH})\text{CH}_2\text{ImMe}]\}(\text{P}^i\text{Pr}_3)_2]\text{OTf}$ (**13**), as a result of the protonation of one of the hydride ligands and the displacement of a coordinated hydrogen molecule of the resulting bis(Kubas-type dihydrogen) intermediate $[\text{Os}(\eta^2\text{-H}_2)_2\{\kappa^2\text{-C,C-}[\text{C}(\text{OH})\text{CH}_2\text{ImMe}]\}(\text{P}^i\text{Pr}_3)_2](\text{OTf})_2$ by one of the $[\text{OTf}]^-$ anions (Scheme 12).

Scheme 12. Preparation of Complex 13



Complex **13** was isolated as a white solid in 76% yield and characterized by X-ray diffraction analysis. The structure has two chemically equivalent but crystallographically independent cations in the asymmetric unit. Figure 5a shows a drawing of one of them. As expected for a saturated d^6 species, the geometry around the osmium atom can be rationalized as a distorted octahedron with *trans*-phosphines ($\text{P1-Os(1)-P(1A)} = 168.55(9)^\circ$ and $167.04(10)^\circ$). The perpendicular plane is formed by the chelate hydroxycarbene-NHC ligand, which acts with C(1)-Os(1)-C(6) bite angles of $79.4(5)^\circ$ and $79.6(5)^\circ$, the coordinated hydrogen molecule situated *trans* to the NHC carbon atom C(1) , and the triflate anion disposed *trans* to the hydroxycarbene carbon atom C(6) ($\text{O(2)-Os(1)-C(6)} = 169.8(4)^\circ$ and $166.9(4)^\circ$). The Os(1)-C(1) distances of 2.093(10) and 2.087(10) Å compare well with those previously reported for other Os-NHC complexes,²³ whereas the Os(1)-C(6) bond lengths of 1.900(12) and 1.919(12) Å support the Os-hydroxycarbene formulation.²⁴ The H(01)-H(02) bond lengths of 0.9(1) and 1.0(1) Å are about 0.35 Å shorter than the separation between H(01) and H(02) in the related phenylpyridine complex **3** and suggest a Kubas-type character for the dihydrogen, which was confirmed by the DFT-optimized structure (Figure 5b). In good agreement with the X-ray diffraction analysis, the DFT calculations yield a H-H distance of 0.853 Å. In the ^1H NMR spectrum, in dichloromethane- d_2 , the coordinated hydrogen molecule displays a broad signal centered at -3.36 ppm. According to a Kubas-type dihydrogen nature, the H-D coupling constant in the partially deuterated species is 29.7 Hz, which allows us to calculate a H-H distance of 0.92 Å.²⁵ The $^{13}\text{C}\{^1\text{H}\}$ NMR spectrum is consistent with the presence of the hydroxycarbene-NHC ligand in the complex. Thus, it contains triplets at 260.1 ($^2J_{\text{C-P}} = 7.6$ Hz) and 170.9 ($^2J_{\text{C-P}} = 8.3$ Hz) ppm for the hydroxycarbene C(6) and

NHC C(1) carbon atoms, respectively. The $^{31}\text{P}\{^1\text{H}\}$ NMR spectrum shows a singlet at 17.9 ppm.

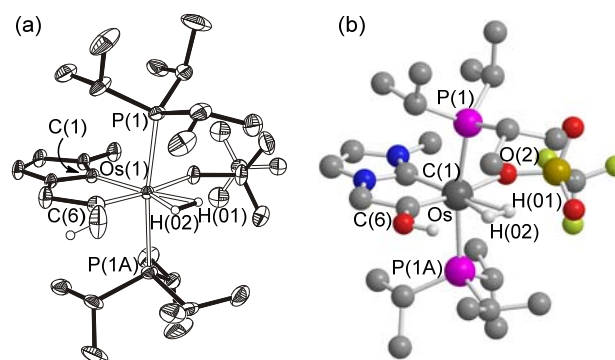


Figure 5. (a) ORTEP diagram of the cation of complex **13** (30% probability ellipsoids). Most hydrogen atoms are omitted for clarity. Selected bond lengths (Å) and angles (deg): $\text{Os(1)-P(1)} = 2.446(2)$, $2.436(3)$, $\text{Os(1)-O(2)} = 2.262(7)$, $2.251(8)$, $\text{Os(1)-C(1)} = 2.093(10)$, $2.087(10)$, $\text{Os(1)-C(6)} = 1.900(12)$, $1.919(12)$, $\text{H(01)-H(02)} = 0.9(1)$, $1.0(1)$; $\text{P(1)-Os(1)-P(1A)} = 168.55(9)$, $167.04(10)$, $\text{C(1)-Os(1)-C(6)} = 79.4(5)$, $79.6(5)$, $\text{C(6)-Os(1)-O(2)} = 169.8(4)$, $166.9(4)$. (b) Optimized structure of the cation of complex **13**. Most hydrogen atoms are omitted for clarity. Selected bond lengths (Å) and angles (deg): $\text{Os-P(1)} = 2.490$, $\text{Os-P(2)} = 2.476$, $\text{Os-C(1)} = 2.077$, $\text{Os-C(6)} = 1.919$, $\text{H(01)-H(02)} = 0.853$; $\text{P(1)-Os-P(2)} = 168.5$, $\text{C(1)-Os-C(6)} = 79.9$.

The low stability of the hydroxycarbene-NHC ligand prevents a more detailed study of the OsH_3 unit of **11**. In order to address this problem, we decided to prepare the methoxycarbene counterpart (Scheme 13). Treatment of dichloromethane solutions of **10** with 1.2 equiv of MeOTf , at room temperature, for 30 min leads to the expected trihydride $[\text{OsH}_3\{\kappa^2\text{-C,C-}[\text{C}(\text{OMe})\text{CH}_2\text{ImMe}]\}(\text{P}^i\text{Pr}_3)_2]\text{OTf}$ (**14**), as a result of the methylation of the acyl group. Complex **14** was isolated as a white solid in 58% yield and characterized by X-ray diffraction analysis.

Scheme 13. Synthesis and Protonation of Complex 14

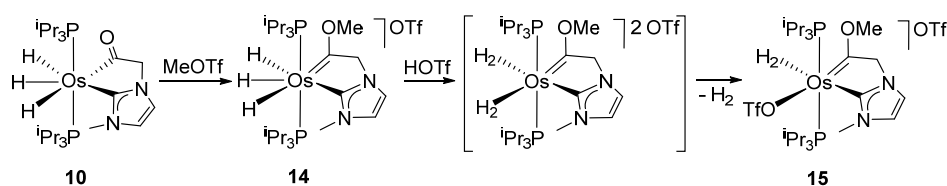


Figure 6a shows a view of the cation of **14**. The coordination geometry around the osmium atom can be rationalized as a distorted pentagonal bipyramid with axial phosphines (P(1)-Os-P(2) = 158.87(2)°) whereas the hydride ligands, separated by 1.52(2) (H(01) and H(02)) and 1.69(3) (H(02) and H(03)) Å, and the methoxycarbene-NHC group, which acts with a C(1)-Os-C(6) bite angle of 77.10(8)°, lie in the perpendicular plane. The Os-NHC and Os-methoxycarbene bond lengths of 2.102(2) (Os-C(1)) and 2.003(2) (Os-C(6)) Å, respectively, compare well with the related parameters of **13**. The classical trihydride nature of this complex was confirmed by the DFT-optimized structure (Figure 6b), which yields separations between the hydrides of 1.634 and 1.769 Å. In agreement with **11**, the high field region of the ¹H NMR spectrum of this trihydride, in dichloromethane-*d*₂, shows a triplet (²*J*_{H-P} = 15.6 Hz) at -8.74 ppm, which displays a 300 MHz *T*₁(min) value of 64 ± 3 ms at 223 K. Although a broadening of this resonance is observed lowering the sample temperature, decoalescence is not observed until 183 K. In the ¹³C{¹H} NMR spectrum, the alcoxycarbene C(6) and NHC C(1) resonances are observed as triplets at 290.8 (²*J*_{C-P} = 3.0 Hz) and 178.2 (²*J*_{C-P} = 6.0 Hz) ppm, respectively. The ³¹P{¹H} NMR spectrum contains a singlet at 31.2 ppm, as expected for equivalent phosphines.

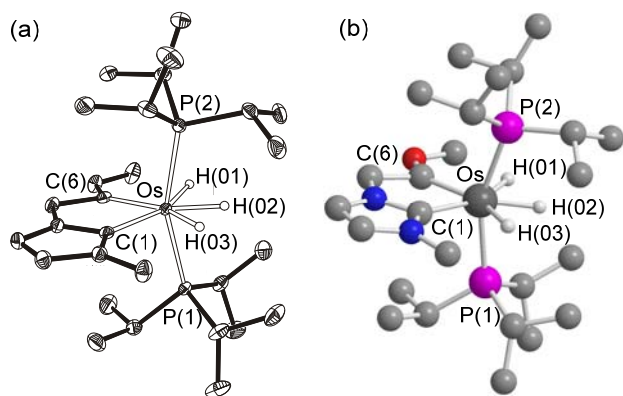


Figure 6. (a) ORTEP diagram of the cation of complex **14** (50% probability ellipsoids). Most hydrogen atoms are omitted for clarity. Selected bond lengths (Å) and angles (deg): Os-P(1) = 2.3825(6), Os-P(2) = 2.3764(6), Os-C(1) = 2.102(2), Os-C(6) = 2.003(2), H(01)-H(02) = 1.52(2), H(02)-H(03) = 1.69(3); P(1)-Os-P(2) = 158.87(2), C(1)-Os-C(6) = 77.10(8). (b) Optimized structure of the cation of complex **14**. Most hydrogen atoms are omitted for clarity. Selected bond lengths (Å) and angles (deg): Os-P(1) = 2.412, Os-P(2) = 2.410, Os-C(1) = 2.125, Os-C(6) = 2.030, H(01)-H(02) = 1.634, H(02)-H(03) = 1.769; P(1)-Os-P(2) = 157.5, C(1)-Os-C(6) = 76.8.

Complexes **11** and **14** are certainly analogous species. The addition of 1.2 equiv of HOTf to the dichloromethane solutions of **14** produces the protonation of a hydride ligand and the formation of the Kubas-type dihydrogen derivative [Os(OTf)(η²-H₂){κ²-C,C-[C(OMe)CH₂ImMe]}(PⁱPr₃)₂][OTf] (**15**), a methoxycarbene counterpart of **13**, which was isolated as white solid in 51% yield. As expected, the spectroscopic data of **15** and **13** are very similar. Thus, the ¹H NMR spectrum of **15**, in dichloromethane-*d*₂, shows the dihydrogen resonance at -3.25 ppm, which displays a 300 MHz *T*₁(min) value of 10 ± 1 ms, at 213 K, whereas the H-D coupling constant in the partially deuterated species is 30.0 Hz. These data are consistent with a H-H distance of 0.93 Å,²⁵ which agrees well with that obtained by DFT calculations for the optimized structure (0.851 Å). In the ¹³C{¹H} NMR spectrum, the resonances corresponding to the metalated carbon atoms of the C₂C-donor ligand appear at 261.7 and 167.3 ppm as triplets with C-P coupling constants of 7.6 and 8.3 Hz, respectively. The ³¹P{¹H} NMR spectrum shows a singlet at 17.9 ppm for the equivalent phosphines.

CONCLUDING REMARKS

There are groups so-called spectator ligands that subtly govern the electron density of the metal, but have not a direct participation in the reactions of polyhydrides of platinum group metals. In spite of the thin borderline between Kubas-type dihydrogen and elongated dihydrogen, it is possible to govern the bis(Kubas-type dihydrogen) or Kubas-type dihydrogen-elongated dihydrogen nature of OsH₄-species with this type of groups. As a proof of concept, here we show that the replacement of the C_{aryl}C_{NHC} chelate ligand of cations [Os(κ²-C_{aryl}C_{NHC})(η²-H₂)₂(PⁱPr₃)₂]⁺ by an orthometalated 2-phenylpyridine, to form [Os{κ²-C,N-(C₆H₄-py)}(η²-H₂)₂(PⁱPr₃)₂]⁺, changes the nature of the Os(η²-H₂)₂ unit from bis(Kubas-type dihydrogen) to Kubas-type dihydrogen-elongated dihydrogen and, as a consequence, there are marked differences in reactivity between them. Particularly, the very different behavior in usual organic solvents should be pointed out.

These [Os(L-L)(η²-H₂)₂(PⁱPr₃)₂]⁺ cations are formed by protonation of classical trihydride complexes OsH₃(L-L)(PⁱPr₃)₂. The presence of a group in the L-L ligand with sufficiently basic free pairs prevents the formation of the Os(η²-H₂)₂ unit because it captures the proton. However, the resulting trihydride containing a chelate HL-L group can be protonated again to now afford an Os(η²-H₂)₂ species. In contrast to [Os{κ²-C,N-(C₆H₄-py)}(η²-H₂)₂(PⁱPr₃)₂]⁺, the reactivity of the new cation reveals a bis(Kubas-type dihydrogen) character for the Os(η²-H₂)₂ unit. The initial protonation of the L-L group reduces its basicity and as a consequence the π-back bonding from the metal to the σ*(HH) orbital, which favors the Kubas-type dihydrogen with regard to an elongated dihydrogen.

In conclusion, the nature and formation of Os(η^2 -H₂)₂ unit of cations [Os(L-L)(η^2 -H₂)₂(PⁱPr₃)₂]⁺ can be subtly tuned with the L-L ligand. Here we report a novel Kubas-type dihydrogen – elongated dihydrogen compound and demonstrate that has a chemical behavior different from that of previously reported bis(Kubas-type dihydrogen) derivatives.

EXPERIMENTAL SECTION

General Information. All reactions were carried out with rigorous exclusion of air using Schlenk-tube techniques. Solvents were obtained oxygen- and water-free from an MBraun solvent purification apparatus. ¹H, ³¹P{¹H}, ¹³C{¹H}, and ¹⁹F{¹H} NMR spectra were recorded on a Varian Gemini 2000, Bruker ARX 300 MHz, Bruker Avance 300 MHz, Bruker Avance 400 MHz or Bruker Avance 500 MHz instrument. Chemical shifts (expressed in parts per million) are referenced to residual solvent peaks (¹H, ¹³C{¹H}), external 85 % H₃PO₄ (³¹P{¹H}), or external CFCl₃ (¹⁹F{¹H}). Coupling constants *J* and *N* are given in hertz. Infrared spectra were recorded on a Perkin-Elmer Spectrum 100 spectrometer as solid films obtained using the attenuated total reflectance (ATR) technique. C, H, N and S analyses were carried out in a Perkin-Elmer 2400 CHNS/O analyzer. High-resolution electrospray mass spectra were acquired using a Micro-TOF-Q hybrid quadrupole time-of-flight spectrometer (BrukerDaltonics, Bremen, Germany). OsH₃{κ²-C,N-(C₆H₄-py)}(PⁱPr₃)₂ (**1**)²⁶ and OsCl{κ²-C,C-[C(O)CH₂ImMe]}(PⁱPr₃)₂ (**9**),¹⁴ were prepared as previously described.

Reaction of OsH₃{κ²-C,N-(C₆H₄-py)}(PⁱPr₃)₂ (1**) with tetrafluoroboric acid: Preparation of [Os{κ²-C,N-(C₆H₄-py)}(η²-H₂)₂(PⁱPr₃)₂]BF₄ (**2**).** A solution of **1** (150 mg, 0.224 mmol) in dichloromethane (10 mL) was treated with 1 equiv of HBF₄·OEt₂ (30 μL, 0.224 mmol) and stirred for 20 min at room temperature, changing the color from bright orange to dark yellow. After this time, the resulting solution was concentrated to ca. 0.5 mL. Diethyl ether (5 mL) was added to afford a yellow solid, which was washed with further portions of diethyl ether (3 x 2 mL) and dried in vacuo. Yield: 144 mg (85%). Anal. calcd. for C₂₉H₅₄BF₄NOsP₂: C, 46.09; H, 7.20; N, 1.85. Found: C, 45.89; H, 7.46; N, 2.03. HRMS (electrospray, *m/z*) calcd. for C₂₉H₅₂NOsP₂ [M - 2H]⁺: 668.3186; found: 668.3183. IR (cm⁻¹): ν(Os-H) 2163 (w), ν(C=C), ν(C=N) 1606 (m), 1584 (m), ν(B-F) 1049 (vs). ¹H NMR (300 MHz, CD₂Cl₂, 233 K): δ 8.85 (d, ³J_{H-H} = 5.9, 1H, H-*arom*), 8.05 (m, 2H, H-*arom*), 7.87 (m, 2H, H-*arom*), 7.23 (m, 3H, H-*arom*), 1.80 (m, 6H, PCH(CH₃)₂), 0.86 (dvt, ³J_{H-H} = 7.1, *N* = 14.1, 36H, PCH(CH₃)₂), -7.21 (br, 4H, Os-H). ¹H NMR (300 MHz, CD₂Cl₂, 183 K, high field region): δ -3.65 (br, 2H, Os-H), -10.96 (br, 2H, Os-H). ¹³C{¹H}-apt NMR (75.42 MHz, CD₂Cl₂, 233 K): δ 164.1 (s, C_{ipso}), 154.2 (s, CH *arom*), 150.5 (t, ²J_{C-P} = 10.7, Os-C), 144.8 (s, C_{ipso}), 144.4, 137.9, 131.3, 126.1, 125.1, 124.2, 121.4 (all s, CH *arom*), 25.0 (vt, *N* = 23.4, PCH(CH₃)₂), 19.8, 19.1 (both s, PCH(CH₃)₂). ³¹P{¹H} NMR (121.4 MHz, CD₂Cl₂, 298 K): δ 13.9 (s). T₁(min) (ms, OsH, 300 MHz, CD₂Cl₂, 243 K): 21 ± 3 (-7.16 ppm).

Reaction of OsH₃{κ²-C,N-(C₆H₄-py)}(PⁱPr₃)₂ (1**) with HOTf: Preparation of Os(H··H){κ²-C,N-(C₆H₄-py)}(OTf)(PⁱPr₃)₂ (**3**).** A solution of **1** (120 mg, 0.179 mmol) in dichloromethane (10 mL) was treated with HOTf (16 μL, 0.179 mmol) and stirred for 20 min at room temperature. After this time, the resulting solution was concentrated to ca. 0.5 mL. Diethyl ether (5 mL) was added to afford a yellow solid, which was washed with further portions of diethyl ether (3 x 2 mL) and dried in vacuo. Yield: 127 mg (87%). Alternatively, this compound can be prepared starting from complex **2**: NaOTf (23 mg, 0.132 mmol) was added to a CH₂Cl₂ solution (8 mL) of **2** (100 mg, 0.132 mmol). After stirring for 1 hour at room temperature, the resulting suspension was filtered through Celite to remove the sodium salts. The solution thus resulting was concentrated to ca. 0.5 mL, and diethyl ether (5 mL) was added to afford a yellow solid, which was washed with further portions of diethyl ether (2 x 2 mL) and dried in vacuo. Yield: 99 mg (92 %). Anal. calcd. for C₃₀H₅₂F₃NO₃OsP₂S: C,

44.16; H, 6.42; N, 1.72; S, 3.93. Found: C, 44.42; H, 6.52; N, 1.76; S, 3.68. HRMS (electrospray, *m/z*) calcd. for C₂₉H₅₂NOsP₂ [M - OTf]⁺: 668.3186; found: 668.3310. IR (cm⁻¹): ν(Os-H) 2161 (w), ν(C=C), ν(C=N) 1605 (m), 1582 (m), ν(C-F) 1299, ν(S-O) 1231, 1209, 1171 (vs). ¹H NMR (300 MHz, CD₂Cl₂, 298 K): δ 9.38 (d, ³J_{H-H} = 5.9, 1H, H-*arom*), 7.99 (d, ³J_{H-H} = 8.2, 1H, H-*arom*), 7.69 (m, 2H, H-*arom*), 7.52 (d, ³J_{H-H} = 7.4, 1H, H-*arom*), 7.23 (m, 1H, H-*arom*), 6.79 (m, 2H, H-*arom*), 2.04 (m, 6H, PCH(CH₃)₂), 1.01 (dvt, ³J_{H-H} = 6.9, *N* = 12.8, 18H, PCH(CH₃)₂), 0.86 (dvt, ³J_{H-H} = 6.9, *N* = 12.8, 18H, PCH(CH₃)₂), -7.04 (t, ³J_{H-P} = 10.6, 2H, Os-H). ¹³C{¹H}-apt NMR (75.42 MHz, CD₂Cl₂, 298 K): δ 164.7 (s, C_{ipso}), 158.8 (t, ²J_{C-P} = 5.5, Os-C), 149.1 (s, CH *arom*), 144.9 (s, CH *arom*), 140.7 (s, C_{ipso}), 136.6, 130.5, 128.6, 124.9, 120.7, 120.2 (all s, CH *arom*), 119.9 (q, ¹J_{C-F} = 316, CF₃), 119.0 (s, CH *arom*), 26.2 (vt, *N* = 23.5, PCH(CH₃)₂), 19.9, 19.7 (both s, PCH(CH₃)₂). ³¹P{¹H} NMR (121.4 MHz, CD₂Cl₂, 298 K): δ 7.6 (s). ³¹F{¹H} NMR (282.3 MHz, CD₂Cl₂, 298 K): δ -78.8 (s). T₁(min) (ms, OsH, 300 MHz, CD₂Cl₂, 213 K): 28 ± 1 (-7.40 ppm).

Reaction of [Os(κ²-C,N-C₆H₄-py)(η²-H₂)₂(PⁱPr₃)₂]BF₄ (2**) with acetone: Preparation of [Os(H··H){κ²-C,N-(C₆H₄-py)}(κ¹-OCMe₂)(PⁱPr₃)₂]BF₄ (**4**).** A solution of **2** (180 mg, 0.238 mmol) in acetone (10 mL) was stirred for 20 min at room temperature. After this time, the resulting solution was concentrated to ca. 0.5 mL. Diethyl ether (5 mL) was added to afford a green solid, which was washed with further portions of diethyl ether (3 x 2 mL) and dried in vacuo. Yield: 180 mg (93%). Anal. calcd. for C₃₂H₅₈BF₄NOsP₂: C, 47.34; H, 7.20; N, 1.73. Found: C, 47.09; H, 7.35; N, 1.90. HRMS (electrospray, *m/z*) calcd. for C₂₉H₅₂NOsP₂ [M - OC(CH₃)₂]⁺: 668.3186; found: 668.3284. IR (cm⁻¹): ν(Os-H) 2176 (w), ν(C=O) 1650 (m), ν(B-F) 1047 (vs). ¹H NMR (300 MHz, CD₂Cl₂, 298 K): δ 9.36 (d, ³J_{H-H} = 5.7, 1H, H-*arom*), 8.13 (d, ³J_{H-H} = 8.3, 1H, H-*arom*), 7.81 (m, 2H, H-*arom*), 7.56 (d, ³J_{H-H} = 7.5, 1H, H-*arom*), 7.40 (t, ³J_{H-H} = 6.5, 1H, H-*arom*), 6.93 (t, ³J_{H-H} = 7.5, 1H, H-*arom*), 6.83 (t, ³J_{H-H} = 7.5, 1H, H-*arom*), 2.43 (s, 6H, O=C(CH₃)₂), 1.79 (m, 6H, PCH(CH₃)₂), 0.97 (dvt, ³J_{H-H} = 6.7, *N* = 13.1, 18H, PCH(CH₃)₂), 0.70 (dvt, ³J_{H-H} = 6.7, *N* = 13.1, 18H, PCH(CH₃)₂), -7.21 (t, ³J_{H-P} = 17.0, 2H, OsH₂). ¹³C{¹H}-apt NMR (75.42 MHz, CD₂Cl₂, 298 K): δ 197.0 (s, OCMe₂), 164.8 (s, C_{ipso}), 154.4 (t, ²J_{C-P} = 7.1, Os-C), 148.0 (s, CH *arom*), 145.6 (s, CH *arom*), 140.6 (s, C_{ipso}), 137.6, 130.8, 125.3, 121.7, 121.4, 120.2 (all s, CH *arom*), 25.7 (vt, *N* = 24.6, PCH(CH₃)₂), 19.8, 19.4 (both s, PCH(CH₃)₂), 18.2 (s, OCMe₂). ³¹P{¹H} NMR (121.4 MHz, CD₂Cl₂, 298 K): δ 6.1 (s). T₁(min) (ms, OsH, 300 MHz, CD₂Cl₂, 213 K): 33 ± 1 (-7.61 ppm).

Reaction of [Os(κ²-C,N-C₆H₄-py)(η²-H₂)₂(PⁱPr₃)₂]BF₄ (2**) with acetonitrile.** A solution of **2** (100 mg, 0.132 mmol) in acetonitrile (10 mL) was stirred for 2 h at room temperature. After this time, the resulting solution was concentrated to ca. 0.5 mL. Diethyl ether (5 mL) was added to afford a white solid, which was washed with further portions of diethyl ether (3 x 2 mL) and dried in vacuo. Yield: 77 mg. ¹H and ³¹P{¹H} NMR spectra recorded in dichloromethane-*d*₂ reveal the presence of the previously reported¹⁸ complexes [OsH(CH₃CN)₃(PⁱPr₃)₂]BF₄ (**5**; δ_{31P} = 19.6 ppm, δ_{1H} hydride region = -15.98 (t, ³J_{H-P} = 19.1)) and [OsH₃(CH₃CN)₂(PⁱPr₃)₂]BF₄ (**6**; δ_{31P} = 26.1 ppm, δ_{1H} hydride region = -12.18 (t, ³J_{H-P} = 11.4)). Integration of the high field resonances in the ¹H NMR spectrum yields a ratio **5**:**6** of 1:8.

Reaction of [Os{κ²-C,N-(C₆H₄-py)}(η²-H₂)₂(PⁱPr₃)₂]BF₄ (2**) with toluene.** A suspension of **2** (100 mg, 0.132 mmol) in toluene (7 mL) was placed in a schlenk flask provided with a Teflon closure and was heated under reflux for 48 h. After this time, an aliquot of the resulting solution was taken and evaporated to dryness. The oily residue obtained was dissolved in 0.5 mL of CD₂Cl₂ and analyzed by NMR spectroscopy. Both ¹H and ³¹P{¹H} NMR spectra confirm the formation of the BF₄⁻ salt of [Os{κ²-C,N-(C₆H₄-py)}(η⁶-toluene)(PⁱPr₃)₂]⁺ (**7**) and the presence of PⁱPr₃.

Reaction of [Os{κ²-C,N-(C₆H₄-py)}(η²-H₂)₂(PⁱPr₃)₂]BF₄ (2**) with *p*-xylene.** A suspension of **2** (100 mg, 0.132 mmol) in *p*-xylene (7 mL) was placed in a schlenk flask provided with a Teflon closure and

2.35–2.20 (m, 6H, PCH(CH₃)₂), 1.24 (dvt, ³J_{H-H} = 7.2, N = 13.8, 18H, PCH(CH₃)₃), 1.03 (dvt, ³J_{H-H} = 7.2, N = 13.8, 18H, PCH(CH₃)₃), -3.36 (br, 2H, OsH₂). ¹³C{¹H}-APT NMR plus HSQC and HMBC (75.5 MHz, CD₂Cl₂, 298 K): δ 260.1 (t, ²J_{C-P} = 7.6, =C(OH)), 170.9 (t, ²J_{C-P} = 8.3, NCN), 126.5 (s, CH_{im}), 119.4 (s, CH_{im}), 70.0 (s, NCH₂), 37.8 (s, NCH₃), 26.5 (vt, N = 25.7, PCH(CH₃)₂), 19.5, 19.1 (both s, PCH(CH₃)₃). ³¹P{¹H} NMR (121.5 MHz, CD₂Cl₂, 298 K): δ 17.9 (s). ¹⁹F{¹H} NMR (282.3 MHz, CD₂Cl₂, 298 K): δ -78.2 (s).

Measurement of the H-D constant in complex 13. A solution of **10** (8 mg, 0.01 mmol) in dichloromethane-*d*₂ (0.5 mL) contained in an NMR tube was treated with DOTf (2.2 μL, 0.025 mmol). Immediately the ¹H and ¹H{³¹P} NMR spectra were recorded, showing the formation of partially deuterated complex **13**. The high field region of the ¹H NMR spectrum showed a multiplet, from which a value of J_{H-D} = 29.7 Hz could be measured.

Reaction of OsH₃{κ²-C,C-[C(O)CH₂ImMe]}(PⁱPr₃)₂ (10**) with MeOTf: Preparation of [OsH₃{κ²-C,C-[C(OMe)CH₂ImMe]}(PⁱPr₃)₂]OTf (**14**).** A solution of **10** (48 mg, 0.075 mmol) in dichloromethane (5 mL) was treated with MeOTf (10.2 μL, 0.090 mmol). The mixture was stirred for 30 minutes and the resulting solution was dried in vacuo, affording a white residue. Addition of diethyl ether (3 mL) afforded a white solid that was washed with further portions of diethyl ether (2 x 3 mL) and finally dried in vacuo. Yield: 35 mg (58%). Anal. Calcd. for C₂₆H₅₅F₃N₂O₄OsP₂S: C, 38.99; H, 6.92; N, 3.50; S, 4.00. Found: C, 38.60; H, 6.57; N, 3.62; S, 4.39. HRMS (electrospray, *m/z*) calcd. for C₂₅H₅₅N₂OOSp₂ [M]⁺: 653.3400; found: 653.3395. ¹H NMR (300 MHz, CD₂Cl₂, 298 K): δ 7.41 (d, ³J_{H-H} = 1.8, 1H, CH_{im}), 7.22 (d, ³J_{H-H} = 1.8, 1H, CH_{im}), 4.34 (s, 3H, OCH₃), 3.91 (s, 3H, NCH₃), 3.64 (s, 2H, NCH₂), 2.06–1.83 (m, 6H, PCH(CH₃)₂), 1.08 (dvt, ³J_{H-H} = 6.9, N = 13.5, 18H, PCH(CH₃)₃), 0.94 (dvt, ³J_{H-H} = 6.9, N = 13.8, 18H, PCH(CH₃)₃), -8.74 (t, ²J_{P-H} = 15.6, 3H, OsH). ¹³C{¹H}-APT NMR plus HSQC and HMBC (75.5 MHz, CD₂Cl₂, 298 K): δ 290.8 (t, ²J_{C-P} = 3.0, =C(OMe)), 178.2 (t, ²J_{C-P} = 6.0, NCN), 125.1 (s, CH_{im}), 118.5 (s, CH_{im}), 74.1 (s, NCH₂), 67.4 (s, OCH₃), 40.0 (s, NCH₃), 30.5 (vt, N = 27.5, PCH(CH₃)₂), 19.7, 19.5 (both s, PCH(CH₃)₃). ³¹P{¹H} NMR (121.5 MHz, CD₂Cl₂, 298 K): δ 31.2 (s). ¹⁹F{¹H} NMR (282.3 MHz, CD₂Cl₂, 298 K): δ -79.0 (s). T₁(min) (ms, OsH₃, 300 MHz, CD₂Cl₂, 223 K): 64 ± 3 (-8.87 ppm).

Reaction of [OsH₃{κ²-C,C-[C(OMe)CH₂ImMe]}(PⁱPr₃)₂]OTf (14**) with HOTf: Preparation of [Os(OTf)(η²-H₂){κ²-C,C-[C(OMe)CH₂ImMe]}(PⁱPr₃)₂]OTf (**15**).** A solution of **14** (100 mg, 0.125 mmol) in dichloromethane (5 mL) was treated with HOTf (13 μL, 0.15 mmol) and the resulting mixture was stirred for 30 min at room temperature. The solution was dried in vacuo, affording a white residue. Addition of diethyl ether (3 mL) afforded a white solid that was washed with diethyl ether (2 x 3 mL) and finally dried *in vacuo*. Yield: 60 mg (51%). Anal. Calcd. for C₂₇H₅₄F₆N₂O₇OsP₂S₂: C, 34.17; H, 5.74; N, 2.95; S, 6.76. Found: C, 34.31; H, 5.88; N, 3.21; S, 6.63. HRMS (electrospray, *m/z*) calcd. for C₂₅H₅₅N₂OOSp₂ [M - OTf + H]⁺: 653.3400; found: 653.3375. ¹H NMR (300 MHz, CD₂Cl₂, 298 K): δ 7.71 (d, ³J_{H-H} = 2.0, 1H, CH_{im}), 7.13 (d, ³J_{H-H} = 2.0, 1H, CH_{im}), 4.15 (s, 3H, OCH₃), 4.05 (s, 3H, NCH₃), 3.43 (t, ⁴J_{P-H} = 3.2, 2H, CH₂), 2.29–2.06 (m, 6H, P-CH), 1.23 (dvt, J_{H-H} = 6.9, N = 13.8, 18H, PCH(CH₃)₃), 1.03 (dvt, J_{H-H} = 6.9, N = 13.8, 18H, PCH(CH₃)₃), -3.25 (br, 2H, OsH₂). ¹³C{¹H}-APT NMR plus HSQC and HMBC (75.5 MHz, CD₂Cl₂, 253 K): δ 261.7 (t, ²J_{C-P} = 7.6, =C(OCH₃)), 167.3 (t, ²J_{C-P} = 8.3, NCN), 125.8 (s, CH_{im}), 120.8 (s, CH_{im}), 68.1 (s, NCH₂), 63.8 (s, OCH₃), 37.5 (s, NCH₃), 26.7 (vt, N = 24.9, PCH), 19.3, 18.7 (both s, PCH(CH₃)₃). ³¹P{¹H} NMR (121.5 MHz, CD₂Cl₂, 283 K): δ 17.9 (s). ¹⁹F{¹H} NMR (282.3 MHz, CD₂Cl₂, 298 K): δ -78.5 (s). T₁(min) (ms, OsH₂, 300 MHz, CD₂Cl₂, 213 K): 10 ± 1 (-3.43 ppm).

Determination of the J_{H-D} value for complex 15. A NMR tube was charged with a solution of **14** (10 mg, 0.012 mmol) in CD₂Cl₂ (0.5 mL). The solution was treated with DOTf (1.3 μL, 0.015 mmol). Immediately, the ¹H and ¹H{³¹P} NMR spectra were recorded, showing the formation of partially deuterated complex **15**. The high field

region of the ¹H NMR spectrum showed a multiplet, from which a value of J_{H-D} = 30 Hz could be measured.

Structural Analysis of Complexes 2, 3, 7, 10, 13 and 14. X-ray data were collected for the complexes on a Bruker Smart APEX DUO (**2, 3, 7** and **10**) or Bruker Smart APEX CCD (**13, 14**) diffractometers equipped with a normal or fine focus respectively, and 2.4 kW sealed tube source (Mo radiation, λ = 0.71073 Å). Data were collected over the complete sphere covering 0.3° in ω at 100±2 K in order to minimize thermal vibration. Data were corrected for absorption by using a multiscan method applied with the SADABS program.²⁷ The structures were solved by Patterson or direct methods and refined by full-matrix least squares on F² with SHELXL2016,²⁸ including isotropic and subsequently anisotropic displacement parameters. The hydrogen atoms were observed in the least Fourier Maps or calculated, and refined freely or using a restricted riding model. The hydrogen atoms coordinated to the metal center were located in the difference Fourier maps. However, its unrestricted refinement systematically ends with distances very close to the metal atoms (~1 Å), totally unreal. To avoid this, the osmium-hydrogen distances were fixed to the average value found in the Cambridge Crystallographic Data Base (DFIX facility, d(Os-H) = 1.59(1) Å), and they were allowed to pivot freely. The disordered groups or solvent molecules were refined with different moieties, restrained geometries, and complementary occupancy factors.

13 was solved and refined in the monoclinic P2₁ and P2₁/m space groups obtaining better results in the latter with two semi-molecules in the asymmetric unit. In this case the distances between the hydride ligands were forced to be the same in the two molecules.

Crystal data for **2**: C₂₉H₅₄NOsP₂, BF₄, M_w 755.68, yellow, irregular block (0.273 x 0.196 x 0.164 mm), orthorhombic, space group Pnma, *a*: 19.619(3) Å, *b*: 15.468(2) Å, *c*: 10.9481(15) Å, *V* = 3322.5(8) Å³, *Z* = 4, *Z'* = 0.5, D_{calc}: 1.511 g cm⁻³, F(000): 1528, T = 100(2) K, μ 3.975 mm⁻¹. 55951 measured reflections (2θ: 3–58°, ω scans 0.3°), 4305 unique (R_{int} = 0.0342); min./max. transm. factors 0.667/0.862. Final agreement factors were R¹ = 0.0271 (3819 observed reflections, I > 2σ(I)) and wR² = 0.0784; data/restraints/parameters 4305/14/200; GoF = 1.091. Largest peak and hole 1.379 (close to osmium atom) and -0.890 e/ Å³.

Crystal data for **3**: C₃₀H₅₂F₃NOsP₂S, M_w 815.92, colorless, irregular block (0.183 x 0.044 x 0.043 mm), orthorhombic, space group Pna2₁, *a*: 30.0687(18) Å, *b*: 10.9235(7) Å, *c*: 10.6026(6) Å, *V* = 3482.5(4) Å³, *Z* = 4, *Z'* = 1, D_{calc}: 1.556 g cm⁻³, F(000): 1648, T = 100(2) K, μ 3.859 mm⁻¹. 34054 measured reflections (2θ: 3–58°, ω scans 0.3°), 8236 unique (R_{int} = 0.0445); min./max. transm. factors 0.667/0.862. Final agreement factors were R¹ = 0.0287 (7115 observed reflections, I > 2σ(I)) and wR² = 0.0566; Flack parameter -0.020(7); data/restraints/parameters 8236/3/389; GoF = 1.047. Largest peak and hole 1.421 (close to osmium atoms) and -0.832 e/ Å³.

Crystal data for **7**: C₂₇H₃₇NOsP, CF₃O₃S, M_w 745.81, green, irregular block (0.140 x 0.065 x 0.046 mm), triclinic, space group P-1, *a*: 9.1148(5) Å, *b*: 12.1341(7) Å, *c*: 13.3669(7) Å, *a*: 96.4830(10)°, *β*: 92.7870(10)°, *γ*: 105.3600(10)°, *V* = 1411.69(13) Å³, *Z* = 2, *Z'* = 1, D_{calc}: 1.755 g cm⁻³, F(000): 740, T = 100(2) K, μ 4.698 mm⁻¹. 18369 measured reflections (2θ: 3–57°, ω scans 0.3°), 6689 unique (R_{int} = 0.0314); min./max. transm. factors 0.694/0.862. Final agreement factors were R¹ = 0.0236 (6094 observed reflections, I > 2σ(I)) and wR² = 0.0513; data/restraints/parameters 6689/0/350; GoF = 1.036. Largest peak and hole 1.230 (close to osmium atoms) and -0.604 e/ Å³.

Crystal data for **10**: C₂₄H₅₂N₂OOSp₂, M_w 636.81, colorless, irregular block (0.218 x 0.068 x 0.059 mm), triclinic, space group P-1, *a*: 8.8452(3) Å, *b*: 11.6878(4) Å, *c*: 14.4791(5) Å, *a*: 76.8795(4)°, *β*: 83.8166(4)°, *γ*: 68.7269(4)°, *V* = 1357.93(8) Å³, *Z* = 2, *Z'* = 1, D_{calc}: 1.557 g cm⁻³, F(000): 648, T = 100(2) K, μ 4.831 mm⁻¹. 16695 measured reflections (2θ: 3–57°, ω scans 0.3°), 6355 unique (R_{int} = 0.0215); min./max. transm. factors 0.628/0.862. Final agreement factors were R¹ = 0.0174 (6138 observed reflections, I > 2σ(I)) and wR² = 0.0408; data/restraints/parameters 6355/0/293; GoF = 1.045. Largest peak and hole 1.284 (close to osmium atoms) and -0.699 e/ Å³.

Crystal data for **13**: C₂₅H₅₂F₃N₂O₄OsP₂S, CF₃O₃S, 0.5(C₄H₁₀O), 0.125(H₂O), M_w 974.26, green, irregular block (0.068 x 0.037 x 0.019 mm), monoclinic, space group P2₁/m, *a*: 9.776(5) Å, *b*: 21.522(11) Å, *c*: 19.764(10) Å, β: 97.227(8)°, *V* = 1695.7(3) Å³, *Z* = 4, *Z'* = 1, D_{calc}: 1.569 g cm⁻³, F(000): 1969, T = 100(2) K, μ 3.339 mm⁻¹. 45049 measured reflections (2θ: 3–57°, ω scans 0.3°), 10956 unique (R_{int} = 0.0910); min./max. transm. factors 0.672/0.862. Final agreement factors were R¹ = 0.0570 (6750 observed reflections, I > 2σ(I)) and wR² = 0.1730; data/restraints/parameters 10956/74/481; GoF = 1.005. Largest peak and hole 1.678 (close to osmium atoms) and -1.636 e/Å³.

Crystal data for **14**: C₂₅H₅₅N₂OOSp₂, CF₃O₃S, M_w 800.92, colorless, irregular block (0.188 x 0.085 x 0.030 mm), triclinic, space group P-1, *a*: 10.1609(11) Å, *b*: 12.1368(13) Å, *c*: 14.3792(15) Å, α: 73.6820(10)°, β: 88.429(2)°, γ: 85.145(2)°, *V* = 1695.7(3) Å³, *Z* = 2, *Z'* = 1, D_{calc}: 1.569 g cm⁻³, F(000): 812, T = 100(2) K, μ 3.964 mm⁻¹. 27625 measured reflections (2θ: 3–57°, ω scans 0.3°), 8746 unique (R_{int} = 0.0295); min./max. transm. factors 0.664/0.862. Final agreement factors were R¹ = 0.0207 (8165 observed reflections, I > 2σ(I)) and wR² = 0.0469; data/restraints/parameters 8746/3/ 375; GoF = 1.040. Largest peak and hole 1.036 (close to the osmium atoms) and -0.659 e/Å³.

ASSOCIATED CONTENT

Supporting Information

The Supporting Information is available free of charge on the ACS publications web site.

NMR spectra of compounds **2–8** and **10–15**, and computational details (pdf).

Cartesian coordinates of the optimized structures (xyz).

Accession codes

CCDC 1580999–1581004 contain the crystallographic data for this paper. These data can be obtained free of charge via www.ccdc.cam.ac.uk/data_request/cif, or by e-mailing data_request@ccdc.cam.ac.uk, or by contacting The Cambridge Crystallographic Data Centre, 12 Union Road, Cambridge CB2 1EZ UK; fax: +44 1223 336033.

AUTHOR INFORMATION

Corresponding Author

* E-mail: maester@unizar.es.

Notes

The authors declare no competing financial interest.

ACKNOWLEDGMENT

Financial support from the MINECO of Spain (Projects CTQ2017-82935-P and Red de Excelencia Consolider CTQ2016-81797-REDC), the Diputación General de Aragón (E-35), FEDER, and the European Social Fund is acknowledged.

REFERENCES

- (1) Esteruelas, M. A.; López, A. M.; Oliván, M. *Chem. Rev.* **2016**, *116*, 8770–8847.
- (2) (a) Kubas, G. J. *Chem. Rev.* **2007**, *107*, 4152–4205. (b) Crabtree, R. H. *Chem. Rev.* **2016**, *116*, 8750–8769.
- (3) On the base of early theoretical results, it was initially concluded that no minimum potential energy corresponding to an elongated dihydrogen structure existed. This prompted to some authors to think that there is only a single type species displaying a continuum of structures with variation of the H–H distances. (See: (a) Heinekey, D. M.; Lledós, A.; Lluch, J. M. *Chem. Soc. Rev.* **2004**, *33*, 175–185. (b) Gelabert, R.; Moreno, M.; Lluch, J. M.; Lledós, A.; Heinekey, D. M.

J. Am. Chem. Soc. **2005**, *127*, 5632–5640). However, subsequent theoretical results revealed that elongated dihydrogen complexes and compressed dihydride derivatives should have different properties, which could be experimentally demonstrated (See: (c) Gelabert, R.; Moreno, M.; Lluch, J. M. *Chem. Eur. J.* **2005**, *11*, 6315–6325).

(4) Eguillor, B.; Esteruelas, M. A.; Lezáun, V.; Oliván, M.; Oñate, E. *Chem. Eur. J.* **2017**, *23*, 1526–1530.

(5) See for example: (a) Espuelas, J.; Esteruelas, M. A.; Lahoz, F. J.; Oro, L. A.; Valero, C. *Organometallics* **1993**, *12*, 663–670. (b) Liu, S. H.; Huang, X.; Lin, Z.; Lau, C. P.; Jia, G. *Eur. J. Inorg. Chem.* **2002**, 1697–1702. (c) Esteruelas, M. A.; Hernández, J. A.; López, A. M.; Oliván, M.; Oñate, E. *Organometallics* **2007**, *26*, 2193–2202. (d) Esteruelas, M. A.; Masamunt, A. B.; Oliván, M.; Oñate, E.; Valencia, M. *J. Am. Chem. Soc.* **2008**, *130*, 11612–11613. (e) Tse, S. K. S.; Bai, W.; Sung, H. H.-Y.; Williams, I. D.; Jia, G. *Organometallics* **2010**, *29*, 3571–3581. (f) Esteruelas, M. A.; García-Raboso, J.; Oliván, M. *Organometallics* **2011**, *30*, 3844–3852. (g) He, G. W. L.; Bai, W.; Chen, J.; Sung, H. H. Y.; Williams, I. D.; Lin, Z.; Jia, G. *Organometallics* **2017**, *36*, 3729–3738.

(6) See for example: (a) Esteruelas, M. A.; Oro, L. A.; Valero, C. *Organometallics* **1992**, *11*, 3362–3369. (b) Castarlenas, R.; Esteruelas, M. A.; Oñate, E. *Organometallics* **2008**, *27*, 3240–3247. (c) Esteruelas, M. A.; Honeczek, N.; Oliván, M.; Oñate, E.; Valencia, M. *Organometallics* **2011**, *30*, 2468–2471. (d) Bertoli, M.; Choualeb, A.; Gusev, D. G.; Lough, A. J.; Major, Q.; Moore, B. *Dalton Trans.* **2011**, *40*, 8941–8949. (e) Esteruelas, M. A.; López, A. M.; Mora, M.; Oñate, E. *ACS Catal.* **2015**, *5*, 187–191. (f) Esteruelas, M. A.; Lezáun, V.; Martínez, A.; Oliván, M.; Oñate, E. *Organometallics* **2017**, *36*, 2996–3004.

(7) See for example: (a) Esteruelas, M. A.; García-Raboso, J.; Oliván, M.; Oñate, E. *Inorg. Chem.* **2012**, *51*, 5975–5984. (b) Esteruelas, M. A.; Oliván, M. *Inorg. Chem.* **2012**, *51*, 9522–9528. (c) Casarrubios, L.; Esteruelas, M. A.; Larramona, C.; Muntaner, J. G.; Oliván, M.; Oñate, E.; Sierra, M. A. *Organometallics* **2014**, *33*, 1820–1833. (d) Casarrubios, L.; Esteruelas, M. A.; Larramona, C.; Lledós, A.; Muntaner, J. G.; Oñate, E.; Ortuño, M. A.; Sierra, M. A. *Chem. Eur. J.* **2015**, *21*, 16781–16785. (e) Casarrubios, L.; Esteruelas, M. A.; Larramona, C.; Muntaner, J. G.; Oñate, E.; Sierra, M. A. *Inorg. Chem.* **2015**, *54*, 10998–11006.

(8) See for example: (a) Crespo, O.; Eguillor, B.; Esteruelas, M. A.; Fernández, I.; García-Raboso, J.; Gómez-Gallego, M.; Martín-Ortiz, M.; Oliván, M.; Sierra, M. A. *Chem. Commun.* **2012**, *48*, 5328–5330. (b) Alabau, R. G.; Eguillor, B.; Esler, J.; Esteruelas, M. A.; Oliván, M.; Oñate, E.; Tsai, J.-Y.; Xia, C. *Organometallics* **2014**, *33*, 5582–5596. (c) Eguillor, B.; Esteruelas, M. A.; Fernández, I.; Gómez-Gallego, M.; Lledós, A.; Martín-Ortiz, M.; Oliván, M.; Oñate, E.; Sierra, M. A. *Organometallics* **2015**, *34*, 1898–1910. (d) Alabau, R. G.; Esteruelas, M. A.; Oliván, M.; Oñate, E.; Palacios, A. U.; Tsai, J.-Y.; Xia, C. *Organometallics* **2016**, *35*, 3981–3995. (e) Alabau, R. G.; Esteruelas, M. A.; Oliván, M.; Oñate, E. *Organometallics* **2017**, *36*, 1848–1859.

(9) (a) Hart, D. W.; Bau, R.; Koetzle, T. F. *J. Am. Chem. Soc.* **1977**, *99*, 7557–7564. (b) Frost, P. W.; Howard, J. A. K.; Spencer, J. L. *J. Chem. Soc., Chem. Commun.* **1984**, 1362–1363. (c) Gross, C. L.; Girolami, G. S. *Organometallics* **2007**, *26*, 160–166. (d) Eguillor, B.; Esteruelas, M. A.; García-Raboso, J.; Oliván, M.; Oñate, E. *Organometallics* **2009**, *28*, 3700–3709. (e) Alós, J.; Bolaño, T.; Esteruelas, M. A.; Oliván, M.; Oñate, E.; Valencia, M. *Inorg. Chem.* **2013**, *52*, 6199–6213.

(10) (a) Werner, H.; Esteruelas, M. A.; Meyer, U.; Wrackmeyer, B. *Chem. Ber.* **1987**, *120*, 11–15. (b) Gross, C. L.; Young, D. M.; Schultz, A. J.; Girolami, G. S. *J. Chem. Soc., Dalton Trans.* **1997**, 3081–3082. (c) Esteruelas, M. A.; Hernández, Y. A.; López, A. M.; Oliván, M.; Oñate, E. *Organometallics* **2005**, *24*, 5989–6000. (d) Webster, C. E.; Gross, C. L.; Young, D. M.; Girolami, G. S.; Schultz, A. J.; Hall, M. B.; Eckert, J. *J. Am. Chem. Soc.* **2005**, *127*, 15091–15101. (e) Gross, C. L.; Girolami, G. S. *Organometallics* **2007**, *26*, 1658–1664.

(11) (a) Castro-Rodrigo, R.; Esteruelas, M. A.; López, A. M.; Oliván, M.; Oñate, E. *Organometallics* **2007**, *26*, 4498–4509. (b) Kuznetsov, V. F.; Gusev, D. G. *Organometallics* **2007**, *26*, 5661–5666. (c)

- Baya, M.; Esteruelas, M. A.; Oliván, M.; Oñate, E. *Inorg. Chem.* **2009**, *48*, 2677-2686. (d) Bolaño, T.; Esteruelas, M. A.; Fernández, I.; Oñate, E.; Palacios, A.; Tsai, J.-Y.; Xia, C. *Organometallics* **2015**, *34*, 778-789.
- (12) (a) Barea, G.; Esteruelas, M. A.; Lledós, A.; López, A. M.; Oñate, E.; Tolosa, J. I. *Organometallics* **1998**, *17*, 4065-4076. (b) Barrio, P.; Esteruelas, M. A.; Oñate, E. *Organometallics* **2002**, *21*, 2491-2503. (c) Barrio, P.; Esteruelas, M. A.; Lledós, A.; Oñate, E.; Tomás, J. *Organometallics* **2004**, *23*, 3008-3015. (d) Barrio, P.; Esteruelas, M. A.; Oñate, E. *Organometallics* **2004**, *23*, 3627-3639. (e) Baya, M.; Eguillor, B.; Esteruelas, M. A.; Lledós, A.; Oliván, M.; Oñate, E. *Organometallics* **2007**, *26*, 5140-5152.
- (13) Grützmacher, H. *Angew. Chem. Int. Ed.* **2008**, *47*, 1814-1818.
- (14) Bolaño, T.; Esteruelas, M. A.; Gay, M. P.; Oñate, E.; Pastor, I. M.; Yus, M. *Organometallics* **2015**, *34*, 3902-3908.
- (15) Ortuño, M. A.; Vidossich, P.; Conejero, S.; Lledós, A. *Angew. Chem. Int. Ed.* **2014**, *53*, 14158-14161.
- (16) The H-H distance was calculated from the $T_1(\text{min})$ value applying the equation $R_{\text{H-H}} = 129.18/r_{\text{H-H}}^6$, where $R_{\text{H-H}} = R_n - R^*$ (R_n is the relaxation rate due to the dipole-dipole interaction, and is equal to $1/T_1(\text{min})$ at 300 MHz, and R^* is the relaxation rate due to all other relaxation contributor of the molecule, and is estimated to be 2.5 s^{-1}). See: Castillo, A.; Esteruelas, M. A.; Oñate, E.; Ruiz, N. *J. Am. Chem. Soc.* **1997**, *119*, 9691-9698.
- (17) Morris, R. H. *Chem. Rev.* **2016**, *116*, 8588-8654.
- (18) (a) Smith, K.-T.; Tilset, M.; Kuhlman, R.; Caulton, K. G. *J. Am. Chem. Soc.* **1995**, *117*, 9473-9480. (b) Esteruelas, M. A.; Fuertes, S.; Oliván, M.; Oñate, E. *Organometallics* **2009**, *28*, 1582-1585.
- (19) (a) Alós, J.; Bolaño, T.; Esteruelas, M. A.; Oliván, M.; Oñate, E.; Valencia, M. *Inorg. Chem.* **2014**, *53*, 1195-1209. (b) Buil, M. L.; Cardo, J. J. F.; Esteruelas, M. A.; Fernández, I.; Oñate, E. *Inorg. Chem.* **2016**, *55*, 5062-5070. (c) Suárez, E.; Plou, P.; Gusev, D. G.; Martín, M.; Sola, E. *Inorg. Chem.* **2017**, *56*, 7190-7199.
- (20) (a) Díez-González, S.; Marion, N.; Nolan, S. P. *Chem. Rev.* **2009**, *109*, 3612-3676. (b) Hindi, K. M.; Panzner, M. J.; Tessier, C. A.; Cannon, C. L.; Youngs, W. J. *Chem. Rev.* **2009**, *109*, 3859-3884.
- (21) (a) See for example: Tan, K. L.; Bergman, R. G.; Ellman, J. A. *J. Am. Chem. Soc.* **2002**, *124*, 3202-3203. (b) Haller, L. J. L.; Page, M. J.; Erhardt, S.; Macgregor, S. A.; Mahon, M. F.; Abu Naser, M.; Vélez, A.; Whittlesey, M. K. *J. Am. Chem. Soc.* **2010**, *132*, 18408-18416. (c) Hu, Y. C.; Tsai, C. C.; Shih, W. C.; Yap, G. P. A.; Ong, T. G. *Organometallics* **2010**, *29*, 516-518. (d) Hatanaka, T.; Ohki, Y.; Tatsumi, K. *Angew. Chem. Int. Ed.* **2014**, *53*, 2727-2729.
- (22) (a) Suggs, J. W.; Jun, C. H. *J. Am. Chem. Soc.* **1984**, *106*, 3054-3056. (b) Rybtchinski, B.; Oevers, S.; Montag, M.; Vigalok, A.; Rozenberg, H.; Martin, J. M. L.; Milstein, D. *J. Am. Chem. Soc.* **2001**, *123*, 9064-9077. (c) Gandelman, M.; Shimon, L. J. W.; Milstein, D. *Chem. Eur. J.* **2003**, *9*, 4295-4300. (d) Bolaño, T.; Buil, M. L.; Esteruelas, M. A.; Izquierdo, S.; Lalrempuia, R.; Oliván, M.; Oñate, E. *Organometallics* **2010**, *29*, 4517-4523.
- (23) See for example: (a) Eguillor, B.; Esteruelas, M. A.; García-Raboso, J.; Oliván, M.; Oñate, E.; Pastor, I. M.; Peñafiel, I.; Yus, M. *Organometallics* **2011**, *30*, 1658-1667. (b) Buil, M. L.; Cadierno, V.; Esteruelas, M. A.; Gimeno, J.; Herrero, J.; Izquierdo, S.; Oñate, E. *Organometallics* **2012**, *31*, 6861-6867. (c) Buil, M. L.; Cardo, J. J. F.; Esteruelas, M. A.; Fernández, I.; Oñate, E. *Organometallics* **2014**, *33*, 2689-2692. (d) Buil, M. L.; Cardo, J. J. F.; Esteruelas, M. A.; Fernández, I.; Oñate, E. *Organometallics* **2015**, *34*, 547-550.
- (24) See for example: (a) Batuecas, M.; Esteruelas, M. A.; García-Yebra, C.; Oñate, E. *Organometallics* **2012**, *31*, 8079-8081. (b) Casanova, N.; Esteruelas, M. A.; Gullías, M.; Larramona, C.; Mascareñas, J. L.; Oñate, E. *Organometallics* **2016**, *35*, 91-99. (c) Buil, M. L.; Cardo, J. J. F.; Esteruelas, M. A.; Oñate, E. *J. Am. Chem. Soc.* **2016**, *138*, 9720-9728.
- (25) $d_{\text{H-H}} = 150 - 1.92J_{\text{H-D}}$. See: Morris, R. H. *Coord. Chem. Rev.* **2008**, *252*, 2381-2394.
- (26) Esteruelas, M. A.; Fernández, I.; Gómez-Gallego, M.; Martín-Ortiz, M.; Molina, P.; Oliván, M.; Otón, F.; Sierra, M. A.; Valencia, M. *Dalton Trans.* **2013**, *42*, 3597-3608.
- (27) Blessing, R. H. *Acta Crystallogr.* **1995**, *A51*, 33-38. *SADABS: Area-detector absorption correction*; Bruker- AXS, Madison, WI, 1996.
- (28) SHELXL 2016/6; Sheldrick, G. M. *Acta Cryst.* **2008**, *A64*, 112-122.

